

Oscillatory regimes in cardiac cells determined by the calcium concentration

Pablo De Ramon,^{*} Sara Iniesta,[†] and Diana Quintana[‡]
(Dated: June 1, 2022)

Spatial and temporal calcium oscillations within cardiac cells can induce spontaneous excitations alien to the normal pace of the heart, favouring the appearance of arrhythmias. In this work we will study the dynamics of this oscillations and the main factors that cause them using multiple mathematical models with the objective of providing insight into the causes of this disorders.

I. INTRODUCTION

Cardiovascular diseases (CVDs) are the leading cause of death globally, representing 32% of all deaths and 38% of premature deaths due to noncommunicable diseases. The causes of CVDs are very diverse, from clogging of the arteries, preventing blood from freely flowing to the heart or brain, to internal bleeding in the brain or the formation of blood clots [1].

A number of this diseases are caused by the loss of rhythm and synchronization in the contraction of cardiac cells from the periodic excitations of the sino-atrial node, the natural cardiac pacemaker, in what are called cardiac arrhythmias, like ventricular tachycardia and atrial and ventricular fibrillation [2].

It is known that calcium plays a major role in the regulation of contraction in cardiac cells, with an increase in its concentration triggering said contraction. In consequence, it has been shown that an incorrect regulation of intracellular calcium levels can result in the appearance of oscillations that induce spontaneous contractions and generate favorable conditions for the onset of arrhythmias [3].

The objective of this paper is studying the main factors that determine the appearance of this calcium oscillations through a series of compartmental cellular models, starting with a four dimensional system in which calcium dynamics are not only simulated in time but also along a spatial dimension. We will continue by simplifying the system removing the spatial dependence on a 3D model, and finally further simplify to a minimal 2D model in which we will show that oscillations are still present under certain conditions.

II. MODELS

In this part of the study we present the different mathematical models used to simulate the evolution of the calcium concentrations in diverse parts of a cardiac cell. This parts of the cell can be represented as different compartments, each one with its own volume, which store and exchange calcium ions (see fig.1). One of the main

compartments that appear in our models is the sarcoplasmic reticulum (SR). The SR is an intracellular organelle that plays a leading role in the regulation of cytosolic calcium during contraction. It pumps calcium from the cytosol into its interior and controls the Ca^{2+} flow in the opposite direction, which produces the cell contraction. This pumping action is achieved thanks to the SR Ca-pump or SERCA (makes Ca^{2+} enter the SR) and the ryanodine receptors or RyR (release the Ca^{2+} to the cytosol). The other main compartment is the cytosol, which simulates the intracellular concentration of calcium far from the SR. Finally, the last compartment is the dyadic space, which acts as an intermediate buffer between the other two and represents the cytosolic space close to the RyR. All models developed are based upon this basic compartment structure.

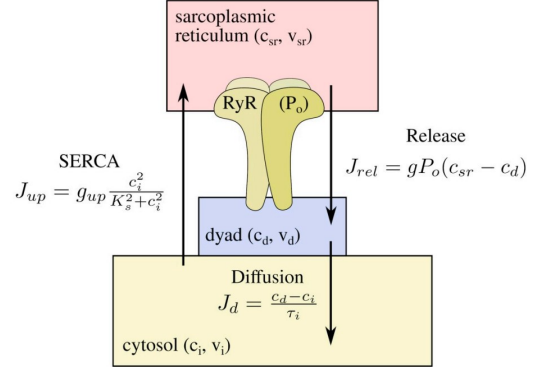


FIG. 1. Schematic view of the compartmental model with the calcium fluxes between them.

A. 4D model: Temporal and spatial evolution of calcium concentrations

The first and most complex model simulates the evolution of the Ca^{2+} concentration in the dyadic space (c_d), the SR (c_{sr}), the cytosol (c_i) and the open probability of the RyR (P_o). The equations for c_d , c_{sr} and P_o dynamics are taken from [3] and the c_i dynamics have been added to complete the model accounting for spatial diffusion

^{*} pablo.de.ramon@estudiantat.upc.edu

[†] sara.iniesta.jovani@estudiantat.upc.edu

[‡] diana.quintana@estudiantat.upc.edu

and conservation of total calcium c_T .

$$\begin{aligned} \frac{dc_d}{dt} &= J_{rel} - J_d \\ \frac{dc_{sr}}{dt} &= \frac{v_i}{v_{sr}} J_{up} - \frac{v_d}{v_{sr}} J_{rel} - J_{sr,diff} \\ \frac{dP_o}{dt} &= k_p c_d^2 (1 - P_o) - k_m P_o \\ \frac{dc_i}{dt} &= \beta(c_i) \left\{ \frac{v_d}{v_i} J_d - J_{up} + J_{i,diff} \right\} \\ J_{rel} &= g P_o (c_{sr} - c_d), \quad J_d = \frac{c_d - c_i}{\tau_i}, \quad J_{up} = g_{up} \frac{c_i^2}{K_s^2 + c_i^2}, \\ \beta(c_i) &= \frac{1}{1 + \frac{B_b K_b}{(K_b + c_i)^2}} \end{aligned}$$

The expressions of J_{rel} , J_{up} and J_d represent the release flux from the SR, the uptake by SERCA and the flux going from the dyadic space to the cytosol due to diffusion (see fig.1). In addition, the constants v_d , v_{sr} and v_i represent the volume of their respective compartments. Details on the rest of the constants can be found in [3].

The terms $J_{sr,diff}$ and $J_{i,diff}$, on the other hand, have been added to the system to introduce the effect of the spatial diffusion of the Ca^{2+} along the length of the one-dimensional SR and cytosol. This way, we are modeling the temporal and spatial evolution of the concentrations. Since we are in 1D, we have discretized the space by distributing equispaced RyR channels in a straight line of $100\mu m$. The diffusion terms will follow Fick's second law in which the temporal evolution of the concentration depends on its second space derivative. The discretization of this term will be the following (general case):

$$\begin{aligned} \frac{\partial c_k}{\partial t} &= D \frac{d^2 c_k}{dx^2} = D \frac{d}{dx} \left(\frac{dc_k}{dx} \right), \quad \frac{dc_k}{dx} \approx \frac{c_{k+1} - c_k}{dx} \\ D \frac{d^2 c_k}{dx^2} &\approx D \frac{\frac{c_{k+1} - c_k}{dx} - \frac{c_k - c_{k-1}}{dx}}{dx} = \frac{D}{(dx)^2} \{c_{k+1} + c_{k-1} - 2c_k\} \end{aligned}$$

with c_k referring to the Ca^{2+} concentration in the k th position of the spatial discretization for the Euler method. Appropriate Dirichlet boundary conditions have been enforced on the system to maintain total calcium concentration constant.

To sum up: we solve the 4D system of ODEs discretizing it both temporally and spatially and using Euler's method in a way that, in every time step, the three concentrations and P_o are calculated for all positions of the RyR channels.

B. 3D model

The 3D model describes the evolution of only c_d , c_{sr} and P_o . Besides, in this model there are no diffusion terms, and the spatial distribution has been removed. Moreover, here the c_i dynamics are not explicitly defined

because this concentration can be computed solving the following conservation equation for the total Ca^{2+} :

$$c_T = \frac{v_i}{v} \left(c_i + \frac{B_b c_i}{K_b + c_i} \right) + \frac{v_d}{v} + \frac{v_{sr}}{v} c_{sr}$$

Therefore, the 3D model will contain three ODEs (c_d , c_{sr} and P_o dynamics), which are the same as the 4D model explained before without $J_{sr,diff}$, and one algebraic equation of Ca^{2+} conservation.

It is important to comment that these last two models are deterministic. However, in our study we wanted to observe which would be the Ca^{2+} evolution for an stochastic RyR open probability.

To solve the 3D model in a different approach than the deterministic one (Euler methods), the open and close dynamics of the RyR were adapted to have a stochastic evolution. At each time step, every channel has a chance of changing states that depends on the open and close rates of the RyR and its comparison with a random number generated by the program. The only possible states for a RyR channel in this model are open and closed, and the P_o is obtained by dividing the number of open gates at a given time step by the total number of gates. This way, the P_o dynamics will no longer have a deterministic evolution, and J_{rel} will be calculated at each time step with the renewed P_o .

C. 2D minimal model

To further reduce the model, we assume that the open and close dynamics of the RyR are much faster than those of the calcium concentration. With this approximation, P_o can be considered as being in a quasi-steady state ($P_o \approx 0$), and can be written in the following way:

$$P_o = \frac{c_d^2}{K_o^2 + c_d^2}$$

Substituting this expression to the 2D ODEs system, we get:

$$\begin{aligned} \frac{dc_d}{dt} &= g \frac{c_d^2}{K_o^2 + c_d^2} - J_d (c_{sr} - c_d) - \frac{c_d - c_i}{\tau_i} \\ \frac{dc_{sr}}{dt} &= \frac{v_i}{v_{sr}} g_{up} \frac{c_d^2}{K_o^2 + c_d^2} - \frac{v_d}{v_{sr}} g \frac{c_d^2}{K_o^2 + c_d^2} (c_{sr} - c_d) \end{aligned}$$

Another approach would be to consider that P_o has a small random fluctuation or noise, such that:

$$P_o = \frac{c_d^2}{K_o^2 + c_d^2} + \sigma(U - 0.5)$$

where σ is the strength of the noise and U is a random uniformly-distributed number between 0 and 1. This expression for P_o is introduced to the 2D ODEs system like before.

Adding noise to the open probability is a simple step towards a more realistic model since, in real systems, the opening and closing of the RyR channels presents intrinsic stochastic dynamics.

III. RESULTS

We will start with our 2D minimal and deterministic model, with the dynamics of c_d and c_{sr} we obtain once we have used the approximation of fast RyR open dynamics. Using the constants of the table in *Supplementary Material* [4], we observe different behaviours depending of the total or average Ca^{2+} concentration in the cell, c_T .

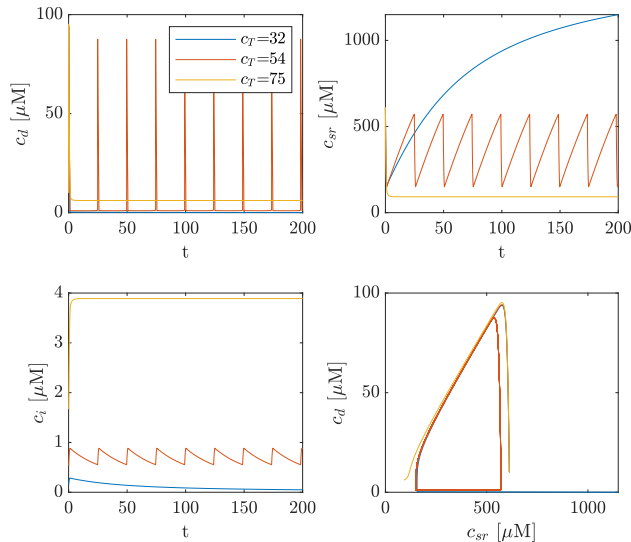


FIG. 2. Time evolution of Ca^{2+} concentration for different values of c_T (2D Model)

As you can see in fig.2, for low Ca^{2+} concentration ($c_T = 32\mu\text{M}$), the system tends to fill the SR compartment and empty the cytosol and dyadic space. In this low concentration steady state, the system is excitable, so if we increase this parameter to $c_T = 75\mu\text{M}$, we find a new fixed point with high c_i and c_d and in which c_{sr} decreases its value compared with the case when $c_T = 32\mu\text{M}$. This makes us believe that, for high values of c_T , most of the Ca^{2+} ions stay in the cytosol and the SR is almost depleted. Although in the figure 2 we see that $c_i = 4\mu\text{M} < c_{sr} \simeq 90\mu\text{M}$, it does not mean that there's more Ca^{2+} ions in the SR, since the volume of the compartments must be taken into account, and the cytosol is much bigger than the SR (see table in [4]). Apart from this two states, we find another one for an intermediate value of the total concentration ($c_T = 54\mu\text{M}$). In this case, the system presents a periodic oscillatory behaviour in all compartments of the cell. In this last oscillatory regime range, it is also observed that the oscillations period grows as the total calcium concentration decreases.

Now we can study the 2D model with noise in P_o . The previous results for different values of c_T showed only one oscillatory state, the one for the intermediate total concentration. In this new model, the results have changed, since we observe oscillations for $c_T=54\mu\text{M}$ and $c_T=32\mu\text{M}$, unlike in the previous case (see annex [4]),

and we have to lower c_T to $20\mu\text{M}$ so that we recover the closed-channels state. The results with noise display also a shorter period than the equivalent without noise. Our results with noise added to the 2D minimal model seem to suggest that allowing the RyRs to behave stochastically could actually increase the c_T parameter region where oscillations appear.

In the second part of the project we studied the 3D model for the same values of c_T . In the first place we plotted the deterministic one (no stochastic effects yet). The difference with this model is that now the open probability of the RyR channels is properly integrated with time. For low total concentration of Ca^{2+} we had

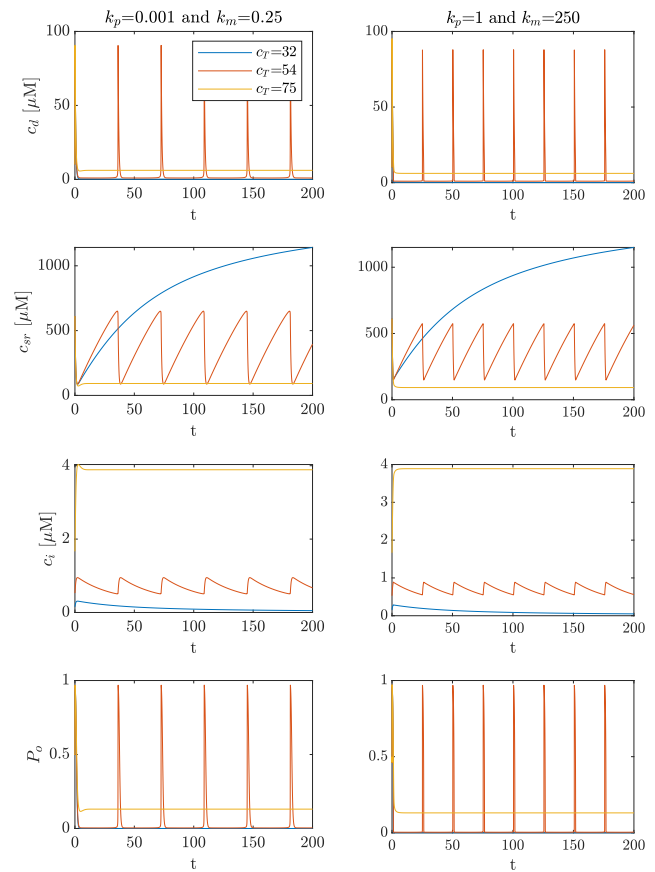


FIG. 3. Time evolution of Ca^{2+} concentration for different values of c_T (3D deterministic model). Normal dynamics (left) and fast P_o dynamics (right).

that c_{sr} increased with the time. This phenomena can now be explained since we can compute how evolves the RyR channels' open probability, which directly affects the concentration of Ca^{2+} in the SR. This probability, for $c_T = 32\mu\text{M}$ is practically zero (is pretty difficult to visualize it in fig.3 even if you expand it). These results are coherent, since having $P_o \approx 0$ means that RyR chan-

nels are closed, no Ca^{2+} is released to the cytosol or dyadic space and the SR is being filled. This is not the case for $c_T = 75\mu\text{M}$, in which $P_o \simeq 0.13$ and there is Ca^{2+} release to the cytosol. The results of this model are qualitatively the same as the 2D (as you can see in fig.2 and 3) for the three different values of c_T . Oscillations also appear for the intermediate state. In fact, since the 2D model was obtained by using the approximation of fast P_o dynamics, if we explicitly change the value of k_p and k_m (which determine the dynamics of P_o) we can obtain the 2D results with the 3D system. In the left column of fig.3 we have used the typical values of these constants. In the right column, on the contrary, we have multiplied both constants for a factor 10^3 to accelerate the dynamics. Doing this we can perceive that the right column plots coincide with the ones in fig.2. In fact, we can check that the periodicity in the 2D oscillatory regime and the one in the right column are the same, which confirms us that the 2D approximation was appropriate.

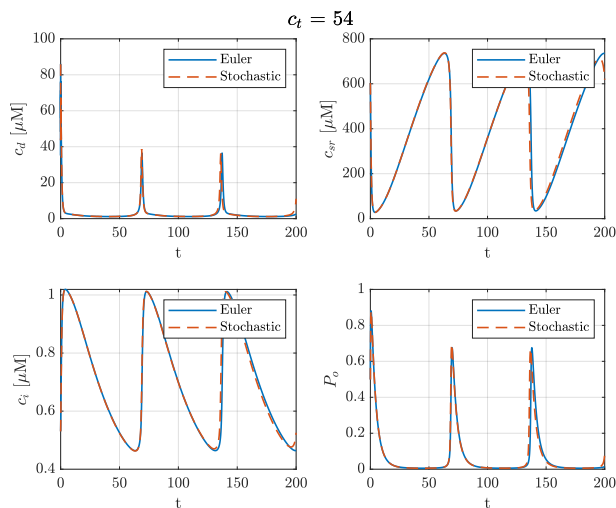


FIG. 4. Comparison between the time evolution of Ca^{2+} concentration and P_o of the stochastic and the deterministic (Euler) 3D model resolution.

In the stochastic resolution of the 3D model, where the RyR dynamics are not deterministically obtained, for a sufficiently large number of channels ($N \gtrsim 10000$), the results coincide almost exactly with those obtained with the full deterministic 3D model (as can be seen in fig. 4 for a c_T of $54\mu\text{m}$). On the other hand, due to the naturally less smooth evolution that has the stochastic open probability compared to the deterministic one, effect that aggravates when having a small number of channels, we are able to observe oscillations appear at a larger range of c_T , just like it happened when we added noise to the 2D model.

To compare the deterministic 4D model with the 3D one, we can compare the 3D results for a given total concentration of Ca^{2+} with the arithmetic average for all channels of the results of the 4D model assigning every

channel the same initial conditions. As can be observed in Fig. 5, both models give the exact same time evolution, just as it happens with other c_T 's. This confirms, once again, that our previous models can be really accurate in the described situations.

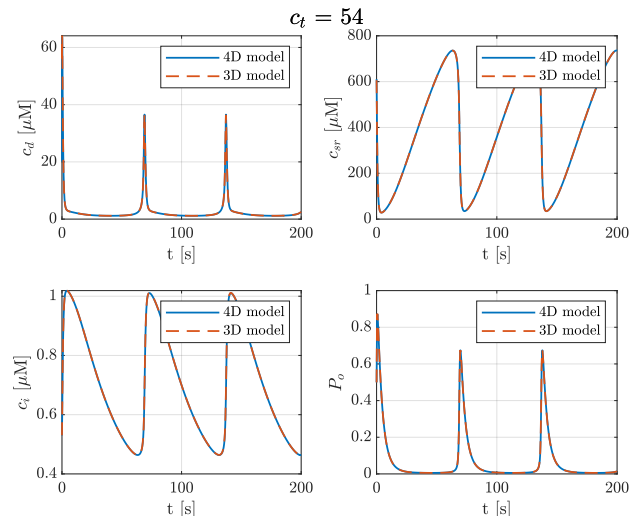


FIG. 5. Comparison between the time evolution of Ca^{2+} concentration and P_o of the deterministic 3D and 4D with constant in space initial conditions model resolution.

IV. CONCLUSION AND DISCUSSION

Calcium ion dynamics are extremely important to understand in order to model the behavior of any muscular tissue, since this ion is crucial for the regulation of its contractile and expansive movements.

By running the simulations and playing with the parameters, we realized that the total concentration of Ca^{2+} in the cell is the most determining parameter between having one or another regime. While lower c_T in the cell does not allow the effective transport of ions through the channels, higher concentrations lead to oscillations in the Ca^{2+} concentration due to the periodic increase in the open probability of the RyR channels or to a permanently open state. A possible consequence of this Ca^{2+} cycling, or directly its entrance in the SR, is the induction of a voltage deflection during the action potential which causes a slowing or reversal of normal repolarization in the cardiac cycle. This would mean that an incorrect balancing of the calcium ions in our body or an incorrect functioning of the implicated channels could lead to consequences such as arrhythmia or even sudden cardiac death [5].

It must also be noted that this models do not take into account the transit of calcium ions between the inside and outside of the cell, so further studies would be needed to obtain more accurate models.

REFERENCES

- [1] Q. Mattingly, *Cardiovascular diseases*, Available at <https://www.who.int/health-topics/cardiovascular-diseases>, World Health Organization, (31/05/2022).
- [2] S. Alonso, M. Bär, and B. Echebarria, “Nonlinear physics of electrical wave propagation in the heart: A review,” *Reports on Progress in Physics*, vol. 79, no. 9, p. 096 601, 2016.
- [3] M. Marchena, B. Echebarria, Y. Shiferaw, and E. Alvarez-Lacalle, “Buffering and total calcium levels determine the presence of oscillatory regimes in cardiac cells,” *PLoS computational biology*, vol. 16, no. 9, e1007728, 2020.
- [4] *Supplementary Material*.
- [5] J. N. Weiss, A. Garfinkel, H. S. Karagueuzian, P.-S. Chen, and Z. Qu, “Early afterdepolarizations and cardiac arrhythmias,” *Heart rhythm*, vol. 7, no. 12, pp. 1891–1899, 2010.